Journal of Dental Sciences

Volume 21 | Issue 2 Article 59

2026

Association of GLI1 overexpression with acanthomatous change in ameloblastoma

Pei-Hsuan Lu

Chih-Huang Tseng

Yi-Ping Wang

Jang-Jaer Lee

Julia Yu-Fong Chang

Follow this and additional works at: https://jds.ads.org.tw/journal

Recommended Citation
Lu, Pei-Hsuan; Tseng, Chih-Huang; Wang, Yi-Ping; Lee, Jang-Jaer; and Chang, Julia Yu-Fong (2026) "Association of GLI1 overexpression with acanthomatous change in ameloblastoma," *Journal of Dental Sciences*: Vol. 21: Iss. 2, Article 59.
Available at: https://jds.ads.org.tw/journal/vol21/iss2/59

This Original Article is brought to you for free and open access by Journal of Dental Sciences. It has been accepted for inclusion in Journal of Dental Sciences by an authorized editor of Journal of Dental Sciences. For more information, please contact cpchiang@ntu.edu.tw.

Available online at https://jds.ads.org.tw/journal/

Digital Commons

journal homepage: https://jds.ads.org.tw/journal/

Original Article

Association of *GLI1* overexpression with acanthomatous change in ameloblastoma

Pei-Hsuan Lu [a,b,c], Chih-Huang Tseng [b,d,e], Yi-Ping Wang [b,c,f], Jang-Jaer Lee [c], Shih-Jung Cheng [c,f], Catherine Huang [g], Hao-Hueng Chang [b,c], Julia Yu-Fong Chang [b,c,f*]

[a] *Department of Dentistry, National Taiwan University Hospital Yunlin Branch, Yunlin, Taiwan*
[b] *Graduate Institute of Clinical Dentistry, School of Dentistry, National Taiwan University, Taipei, Taiwan*
[c] *Department of Dentistry, National Taiwan University Hospital, College of Medicine, National Taiwan University, Taipei, Taiwan*
[d] *Division of Oral Pathology & Maxillofacial Radiology, Kaohsiung Medical University Hospital, Kaohsiung, Taiwan*
[e] *Oral & Maxillofacial Imaging Center, College of Dental Medicine, Kaohsiung Medical University, Kaohsiung, Taiwan*
[f] *Graduate Institute of Oral Biology, School of Dentistry, National Taiwan University, Taipei, Taiwan*
[g] *Stanford University, Stanford, CA, USA*

Received 30 December 2025
Available online 1 April 2026

KEYWORDS
Ameloblastoma;
MAPK pathway;
SHH pathway;
BRAF V600E mutation;
GLI1;
CK17

Abstract *Background/purpose:* Mutations in mitogen-activated protein kinase (MAPK) and sonic hedgehog (SHH) pathways are the most common genetic changes reported in ameloblastomas. This study tried to find the mutational landscape of ameloblastomas in Taiwan and clarify the role of SHH pathway in the pathogenesis of ameloblastoma.
Materials and methods: Sanger sequencing of the mutation hot spots in *BRAF*, *KRAS*, *FGFR2*, and *SMO* genes were performed in 77 ameloblastomas. Real-time RT-PCR and double immunohistochemistry were performed for measurement of glioma-associated oncogene homolog 1 (*GLI1*) mRNA expression levels and detection of GLI1 protein and cytokeratin 17 (CK17) expressions in 30 ameloblastomas, respectively.
Results: BRAF V600E mutations were identified in 77.9 % (60/77) ameloblastomas. No *FGFR2 (C382R), KRAS (G12R),* or *SMO (L412F or W535L)* mutation could be identified in this cohort. *GLI1* mRNA expression in ameloblastoma was significantly associated with older age of the patient, recurrent tumor, and keratin formation. Furthermore, significantly higher *GLI1* mRNA expression level in acanthomatous ameloblastomas than controls and other histological

* Corresponding author. Department of Dentistry, National Taiwan University Hospital, College of Medicine, National Taiwan University, No. 7, Chung Shan S. Rd., Zhongzheng Dist., Taipei 100, Taiwan.
E-mail address: jyfchang@ntu.edu.tw (J.Y.-F. Chang).

https://doi.org/10.1016/j.jds.2026.01.002
1991-7902/© 2026 Association for Dental Sciences of the Republic of China. Publishing services by Digital Commons. This is an open access article under the CC BY-NC-ND license (http://creativecommons.org/licenses/by-nc-nd/4.0/).

subtypes of ameloblastomas, indicating a positive correlation between the *GLI1* mRNA expression level and keratin formation in ameloblastomas. The double immunostains demonstrated the juxtaposition, instead of co-localization, of GLI1 and CK17 expression in the ameloblastoma tumor nest, suggesting a paracrine control of keratin production by the GLI1 protein in ameloblastoma.

Conclusion: The concomitant activation of both the MAPK and SHH pathways is frequently found in ameloblastomas. GLI1 may stimulate the keratin production through a paracrine regulatory mechanism. SHH pathway is most likely a later event in the pathogenesis of ameloblastomas.

© 2026 Association for Dental Sciences of the Republic of China. Publishing services by Digital Commons. This is an open access article under the CC BY-NC-ND license (http://creativecommons.org/licenses/by-nc-nd/4.0/).

Introduction

Ameloblastoma is the most common benign odontogenic neoplasm and is characterized by locally aggressive behavior and a high recurrence rate.[1,2] Consequently, wide surgical resection is the recommended treatment, frequently resulting in significant functional and esthetic impairment of the craniofacial complex. Although multiple genetic alterations in ameloblastomas have been identified recently,[3–6] the knowledge of pathogenesis of ameloblastoma remains limited. Elucidation of the cellular and molecular mechanisms underlying the pathogenesis of ameloblastoma is therefore critical for the advancement of targeted and less morbid therapeutic strategies.

According to the 2023 World Health Organization (WHO) classification, ameloblastomas are categorized based on locations and histopathology as solid/multicystic (92 %), unicystic (6 %), and extra-osseous (2 %).[1] Histopathologically, six subtypes of ameloblastoma are recognized: follicular, plexiform, acanthomatous, granular cell, desmoplastic, and basal cell types. Notably, these histologic patterns demonstrate preferential anatomic distribution and distinct genetic alterations.[6] Follicular types occur more frequently in the mandible and are associated with *BRAF V600E* mutation, whereas plexiform types are more often found in the maxilla and have been linked to *SMO* mutations.[6] However, the subsequent larger studies have suggested that tumor location (mandible vs. maxilla) correlates more strongly with mutation profiles than histologic subtype, with *BRAF* mutations predominating in the mandibular and non-plexiform tumors.[3,4] In addition to *BRAF* and *SMO* mutations, few mutations in *KRAS, NRAS, HRAS, FGFR2, PI3KCA, CTNNB1, and SMARCB1* have also been reported.[4,6]

Early studies suggested that *BRAF* and *SMO* mutations were nearly mutually exclusive, implying two independent molecular pathways in ameloblastoma tumorigenesis.[6] However, subsequent large-scale analyses demonstrated frequent coexistence of *SMO* mutations with alterations in *RAS* and *FGFR2*,[3] and occasional overlap with *BRAF* mutation (37 %, 32 % and 16 % of *SMO* mutated cases, respectively).[3] Given the substantially higher overall mutation rates within the FGFR2-RAS-BRAF-MAPK pathway (approximately 88 %) compared with *SMO* mutations (16 %—39 %), and the frequent coexistence of *SMO* mutations with MAPK pathway alterations (85 % of *SMO* mutated cases), it has been proposed that MAPK pathway activation represents a primary oncogenic driver, whereas sonic hedgehog (SHH) pathway activation may occur as a later event.[3]

Clinically, several case reports and small series have demonstrated encouraging responses to MAPK pathway inhibitors in patients with *BRAF*-mutated ameloblastomas.[7–11] Nevertheless, residual tumors,[7–11] squamous differentiation following therapy,[8,10,11] tumor recurrence or relapse,[9,10] resistance to MEK inhibitor,[12] and *in vitro* resistance to BRAF inhibitors have all been reported,[13] underscoring the need for a more comprehensive understanding of the pathway interactions in ameloblastoma.

In the present study, we aimed to characterize the mutation profile of ameloblastomas in Taiwan and to further elucidate the role of the SHH pathway in their pathogenesis. Although *BRAF V600E* mutation was identified in majority of cases, no mutations in *FGFR2, KRAS* or *SMO (L412F or W535L)* were detected. We therefore investigated *GLI1*, the key downstream transcription factor of the SHH pathway, at both the mRNA and protein levels. We further explored the relationship between GLI1 expression and keratin production using cytokeratin 17 (CK17) as a marker. Our findings provided evidence for the concomitant activation of MAPK and SHH pathways and suggested that SHH signaling might represent a late, progression-associated event in ameloblastoma.

Materials and methods

Clinical samples

Non-decalcified formalin-fixed paraffin-embedded (FFPE) samples from 77 ameloblastomas (30 follicular, 19 plexiform, 25 unicystic, two granular cell, and one desmoplastic types) were included. One syndromic odontogenic keratocyst (OKC), one calcifying odontogenic cyst (COC) and four radicular cysts used as positive or negative controls were also included. All cases were diagnosed at National Taiwan University Hospital (NTUH) between 2007 and 2016. Clinical data, including age, gender, root resorption, recurrent history, and follow-up information were collected.

Keratinized areas were quantified using ImageJ.[14] This study was approved by the Research Ethics Committee of NTUH (No. 201412058RINA, 201608088RINA, and 201901034RIND).

DNA and RNA extraction

Tumor areas were macrodissected from two to five 10 μm-thick FFPE sections, ensuring more than 80 % tumor content. DNA and RNA were sequentially extracted using the AllPrep® DNA/RNA FFPE Kit (Qiagen, Hilden, Germany) according to the manufacturer's instructions. Nucleic acid concentrations were measured using a Nanodrop Lite spectrophotometer (Thermo Fisher Scientific, Waltham, MA, USA).

PCR and sanger sequencing

Hot-start PCR was performed using AmpliTaq Gold polymerase (Thermo Fisher Scientific) to amplify *BARF V600E*, *FGFR2 (C382R)*, *KRAS (G12R)*, and *SMO (L412F, W535L)*. The following primers were used: *BRAF* (600)-F-TGCTTGCTCT GATAGGAAAATG; *BRAF* (600)-R-AGCATCTCAGGGCCAAAAAT; *SMO* (412)-F-GATGGGGACTCTGTGAGTGG; *SMO* (412)-R-T GTTGCCCAACTGGTCCT; *SMO* (412)-nested-F-GGGATTT GTTTT GTGGGCTA; *SMO* (412)-nested-R-GCCTGGTCTTCACT CACCTC; *SMO* (535)-F-CCCATCCCTGACTGTGAGAT; *SMO* (535)-R-CAGGTACGCCTCCAGATGAG; *KRAS* (12)-F-TTTATTAT AAGGCCTGCTGAAAATG; *KRAS* (12)-R-AGAATGGTC CT GCACCAGTAATA; *FGFR2* (382)-F-TCGGCACAGGATGACTGTT A; *FGFR2* (382)-R-AATCTAGCGCCTGGAAGAGA. The PCR temperature settings were as follows: 95 °C for 5 min and then 30 s in each cycle for denaturation, temperature increase from 50 °C to 60 °C (according to the melting temperatures of the specific primers) for 30 s for annealing, and 72 °C for 30 s for extension. The PCR products were purified with Rapid PCR cleanup Enzyme Set (New England BioLabs, Ipswich, MA, USA) and sequenced at the NTUH Sequencing Core Facility.

Quantitative real-time RT-PCR

Thirty ameloblastomas with sufficient RNA quality (12 follicular, 6 plexiform and 12 unicystic cases), along with control lesions, were analyzed. cDNA was synthesized using a High-Capacity Reverse Transcription Kit (Thermo Fisher Scientific). *GLI1* expression was quantified using TaqMan assays, normalized to *β-actin* (Hs00171790_m1 and Hs99999903_m1; Thermo Fisher Scientific), and expressed relative to the COC sample.

Double immunohistochemistry for GLI1 protein and CK17

Double immunohistochemical staining for the GLI1 and CK17 was performed on 4-μm FFPE sections using a Ventana Benchmark XT autostainer. Antibodies included rabbit polyclonal antibody against the GLI1 protein (1:400 dilution, Novus Biologicals, LLC, Centennial, CO, USA) and a mouse monoclonal antibody against the CK17 (1:40 dilution, clone E3, DAKO, Agilent Technologies, Santa Clara, CA, USA).

Statistical analysis

Associations between *GLI1* expression and clinicopathological parameters were evaluated using Mann–Whitney U and linear regression tests. Statistical analyses were conducted using IBM SPSS Statistics for Windows, Version 20.0 (IBM Corp., Armonk, NY, USA). The *P*-value <0.05 was considered to be significant.

Results

BRAF V600E mutations were identified in 60 of 77 ameloblastomas (77.9 %). Mutation frequencies were 83.3 % (25/30) in follicular, 78.9 % (15/19) in plexiform, 76.0 % (19/25) in unicystic, and 50.0 % (1/2) in granular cell types, whereas the desmoplastic case was wild type (Table 1). No *FGFR2 (C382R)*, *KRAS (G12R)*, or *SMO (L412F or W535L)* mutations were detected.

GLI1 mRNA expression was significantly higher in ameloblastomas than in negative control lesions ($P = 0.002$) (Fig. 1; Table 2). Some of the ameloblastoma cases even showed higher *GLI1* expression than the syndromic OKC case. Expression levels varied among histologic subtypes ($P = 0.014$) and were significantly higher in solid/multicystic tumors ($P = 0.016$, Fig. 2), older patients ($P = 0.004$), and recurrent cases ($P = 0.005$). No significant associations were observed with root resorption, bone perforation, tumor location, or BRAF mutation status (Fig. 2).

Interestingly, the higher *GLI1* mRNA expression level was found in acanthomatous ameloblastomas than in other

Table 1 Data summarize the *BRAF V600E* mutation status and ameloblastoma subtypes.

Ameloblastoma subtype	*BRAF* Wild type	*BRAF V600E* Mutant type	Total numbers of cases	Mutation rate
Follicular	5	25	30	83.3 %
Plexiform	4	15	19	78.9 %
Unicystic	6	19	25	76.0 %
Granular	1	1	2	50.0 %
Desmoplastic	1	0	1	0 %
Total	17	60	77	77.9 %

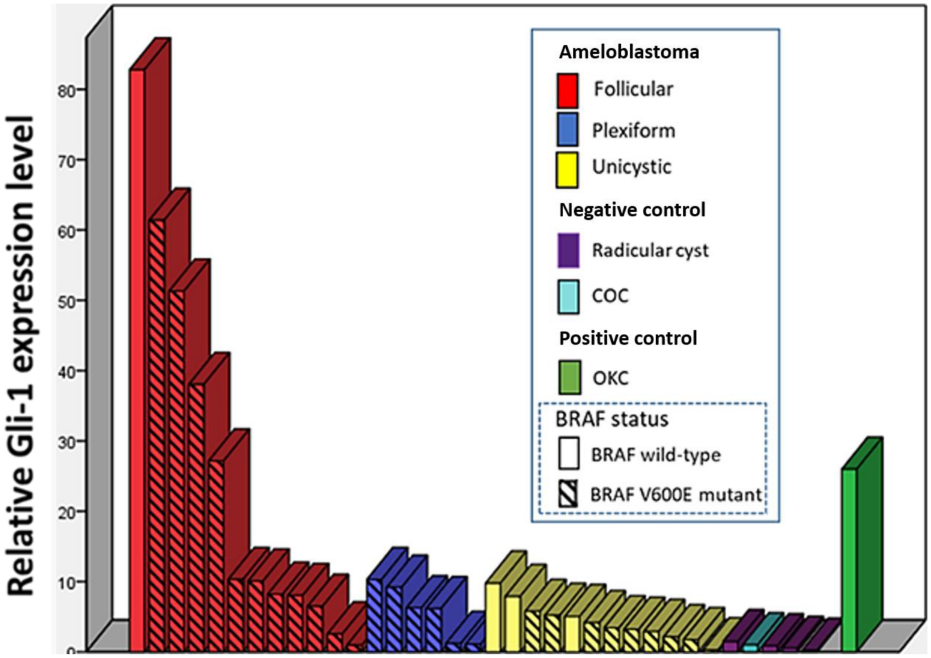

Figure 1 Relative *GLI1* mRNA expression level and *BRAF* mutation status in 30 ameloblastomas, one calcifying odontogenic cyst (COC), four radicular cysts, and one syndromic odontogenic keratocyst (OKC).

Table 2 Statistical analysis of relative *GLI1* mRNA expression level according to the clinicopathological parameters.

Relative *GLI1* mRNA expression level	Ameloblastoma vs. negative control	Ameloblastoma subtype		Age (≤20 vs. 21-44 vs. ≥45)	Recurrent vs. non-recurrent	*BRAF* mutation status Gender Root resorption Bone perforation Post-operation prognosis
		Follicular vs. plexiform vs. unicystic	Solid multicystic vs. unicystic			
[a]*P*-value	0.002	0.014	0.016	0.004	0.005	>0.05

[a] Mann—Whitney U test.

histological types of ameloblastomas. This finding indicates a positive correlation between the *GLI1* mRNA expression level and keratin production in ameloblastomas. To verify our findings, the areas of keratin products were calculated and the relationship between *GLI1* mRNA expression level and the amount of keratin was analyzed. Representative six ameloblastoma cases with the highest and lowest *GLI1* expression levels were shown in Fig. 3. The linear regression model revealed the high correlation coefficient ($R = 0.919$) and a significant positive correlation ($P = 0.01$) between the *GLI1* mRNA expression level and the keratin production in the ameloblastomas.

To elucidate whether the GLI1 expressing cells are keratin producing cells, the double immunohistochemical stains for the GLI1 protein and CK17 were performed. A syndromic OKC was served as the positive control and revealed strong brown nuclear staining of GLI1 protein in the basal cells of the lining epithelium and red cytoplasmic staining of CK17 in lining epithelial cells from the suprabasal to keratin layer (Fig. 4A). In contrast, a radicular cyst was used as negative control and revealed weak GLI1 protein expression and absence of CK17 staining in the non-keratinized stratified squamous lining epithelial cells (Fig. 4B). Adding secondary antibody without primary antibody was used as negative control (Fig. 4C).

By the double immunostains for the GLI1 protein and CK17, these 30 FFPE ameloblastoma samples showed various densities and numbers of GLI1 protein-positive brown nuclear staining and CK17-positive red cytoplasmic staining in ameloblastoma cells (Fig. 5A—F). The plexiform type ameloblastoma revealed less GLI1 protein-positive cells and scanty to weak CK17 positive cells (Fig. 5A) than in follicular type ameloblastoma (Fig. 5B—F). The GLI1 protein was expressed mainly in the peripheral cells of ameloblastoma tumor nests and the CK17 expression was mainly detected in the central acanthomatous cells and keratin pearls of ameloblastoma tumor nests (Fig. 5B—F). The CK17 expression in the central acanthomatous cells was commonly

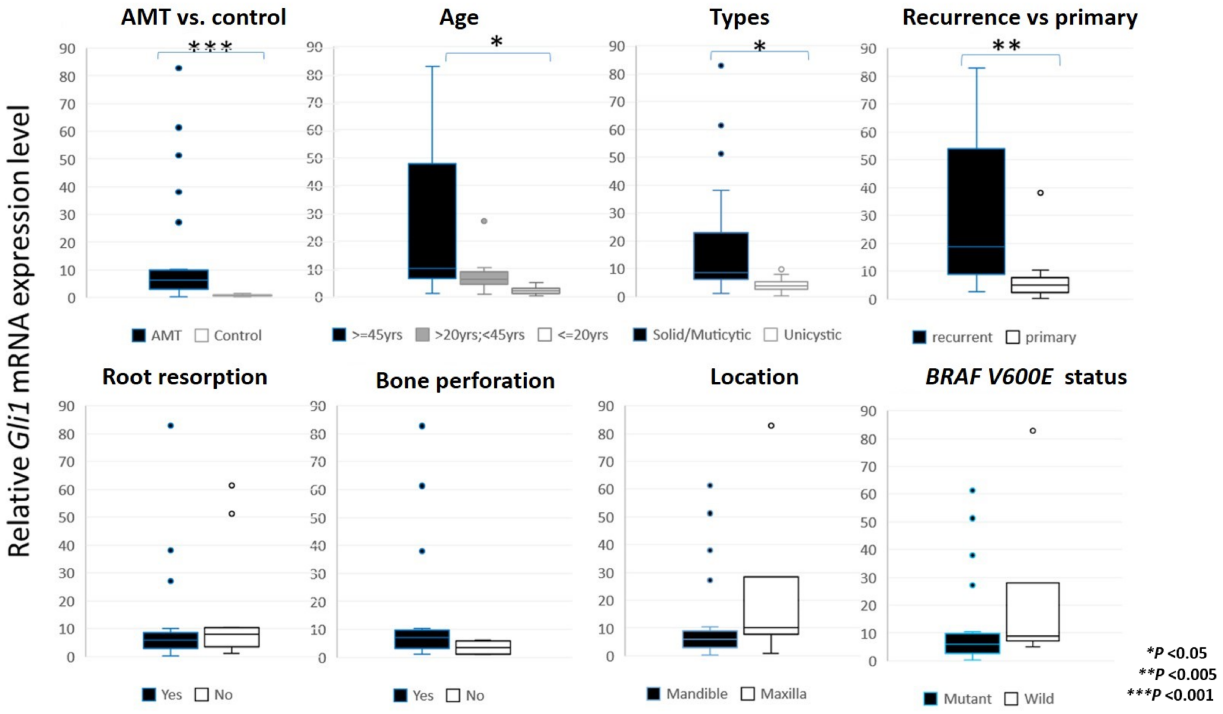

Figure 2 Relative *GLI1* mRNA expression in ameloblastoma (AMT) according to clinicopathologic parameters. Box-and-whisker plots demonstrated relative *GLI1* mRNA expression levels in ameloblastoma tissues compared with control odontogenic tissues (AMT vs. control), stratified by patient age, histologic subtype, tumor status (primary vs. recurrent), root resorption, bone perforation, tumor location, and *BRAF V600E* mutation status. GLI1 expression was significantly higher in ameloblastoma than in control tissues and showed significant associations with older patient age, solid/multicystic histologic type, and recurrent tumors. No statistically significant differences were observed with respect to root resorption, bone perforation, tumor location, or *BRAF V600E* mutation status. Boxes represent the interquartile range, the central line indicates the median, whiskers denote the minimum and maximum values, and dots indicate individual outliers. Statistical significance is indicated as $*P < 0.05$, $**P < 0.005$, and $***P < 0.001$.

accompanied with the GLI1 protein expression in the peripheral cells of the same ameloblastoma tumor nests but there was rare co-localization of both GLI1 protein and CK17 in the same individual ameloblastoma cells (Fig. 5B–F).

Discussion

This study identified a high prevalence of *BRAF V600E* mutations in ameloblastomas from Taiwan. Although the observed mutation rate was higher than that reported in earlier studies, 3,6,15,16 which showed an average prevalence of 62.7 %, as ethnicity has been shown to influence the prevalence of ameloblastomas,[17–19] and the present findings were consistent with findings from other East Asian populations.[20–22] The absence of *FGFR2*, *RAS*, and *SMO* mutations may reflects, at least in part, the predominance of the mandibular lesions in this cohort, as well as the ethnic factors.

In our series, no *SMO (L412F or W535L)* mutation could be detected in 77 ameloblastomas. However, our ameloblastomas demonstrated a significantly higher *GLI1* mRNA expression level than the COC and radicular cysts and *GLI1* mRNA expression level was unrelated to the *BRAF* mutation status. The frequent overexpression of *GLI1* mRNA in ameloblastomas supports the hypothesis that activation of the SHH pathway still plays a role in the pathogenesis of ameloblastoma even without *SMO* mutation. Moreover, the *GLI1* mRNA overexpression is significantly higher in solid/multicystic type than unicystic type ameloblastomas ($P = 0.016$). This result is similar to the study of Gültekin et al.,[23] which showed that in 57 ameloblastomas, eight *SMO* mutations are found in plexiform and mixed types and no *SMO* mutation can be detected in unicystic type ameloblastoma. Interestingly, we discovered that the *GLI1* mRNA overexpression was significantly associated with ameloblastomas in elder patients ($P = 0.004$) and recurrent ameloblastomas ($P = 0.005$), indicating that the *GLI1* mRNA overexpression and the concomitant activation of the SHH pathway may be a late event in the pathogenesis of ameloblastoma, which supports the theory held by Brown et al.[4] Although Sweeney et al.[6] stated that activating MAPK pathway and *SMO* mutations in the SHH pathway represent two molecular subclasses of ameloblastoma. In their research, 8 of the 11 *SMO* mutations still coexist with genetic alterations in the MAPK pathway (3 cases with *RAS*, 3 cases with *FGFR2*, and 2 cases with *BRAF* mutations). Even though no mutation can be identified in the MAPK pathway for the 3 ameloblastomas with *SMO* mutation solely,[6] the activation of MAPK pathway is still possible present through the EGFR overexpression, which has been shown in Kurppa et al.'s study.[16] However, it is still possible that the

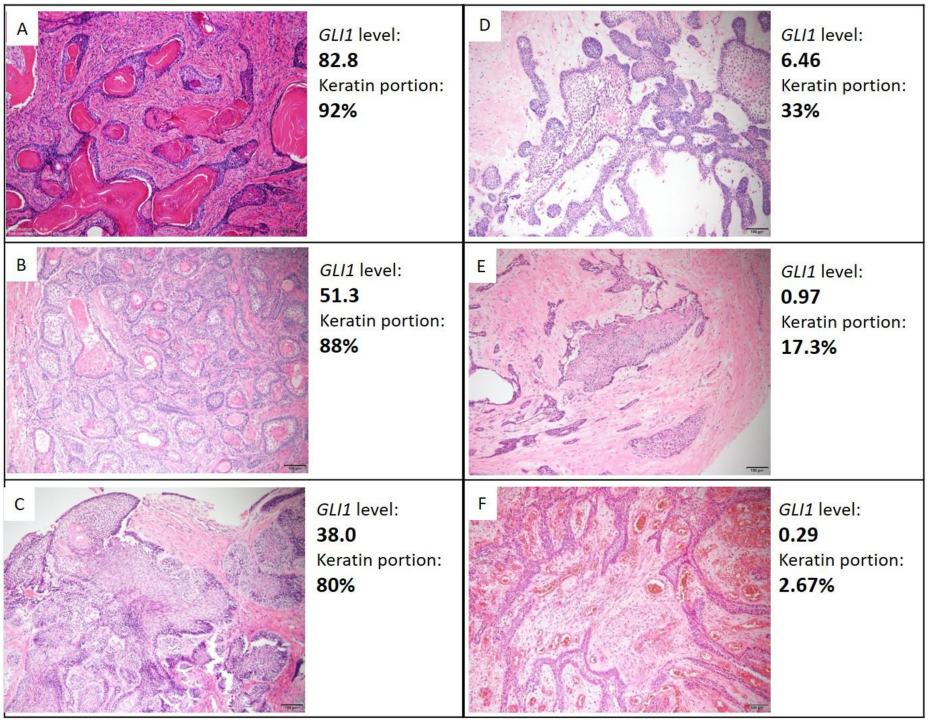

Figure 3 Histopathologic microphotographs of the representative cases showing the correlation between keratin production and *GLI1* mRNA expression level. The portion of keratin production in the ameloblastoma tumor nests had positive correlation with the *GLI1* mRNA expression level ($R = 0.919$, $P = 0.01$). The higher *GLI1* mRNA expression level could be detected in ameloblastomas with more keratin production than in ameloblastomas with less keratin production. (Original magnification; A-F, 100 $\times$).

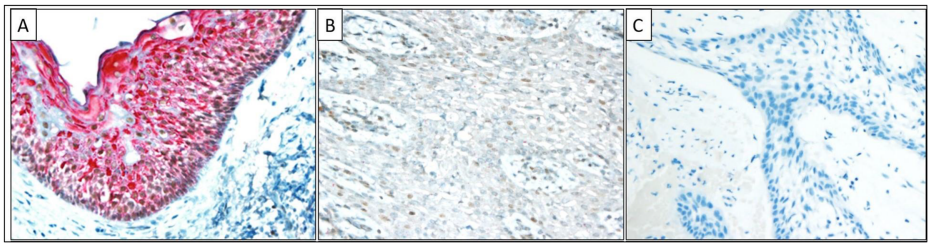

Figure 4 Double immunohistochemical staining for GLI1 protein and CK17 in positive and negative controls. (A) Positive control of a syndromic odontogenic keratocyst showing the GLI1 protein-positive brown nuclear staining in the basal cells of the lining epithelium and the CK17-positive red cytoplasmic staining in the suprabasal and spinous cells of the lining epithelium. (B) Negative control of a radicular cyst demonstrating the GLI1 protein-positive weak brown nuclear staining and none of the CK17-positive red cytoplasmic staining in the stratified squamous lining epithelial cells. (C) No primary antibody negative control showing no GLI11 brown nuclear staining and CK17 red cytoplasmic staining. (Original magnification; A-C, 400 $\times$).

pathogenesis related to SMO mutation and activation of SHH pathway through GLI1 overexpression is different. Further studies to elucidate this question are still needed.

The previous studies showed that the GLI1 protein may mediate CK 17 expression in oral squamous cell carcinoma (OSCC) due to unknown mechanisms.[24] Our study also revealed a positive correlation between the GLI1 protein expression and keratin production in the tumor nests of ameloblastomas. Although a high level of *GLI1* mRNA expression was found in acanthomatous ameloblastomas, the double immunohistochemical stains for the Gli1 protein and CK17 showed no co-localization of the Gli1 protein and CK17 expressing cells in the majority of the ameloblastoma tumor cells. Our results suggest that the GLI1 protein may regulate CK17 expression by a paracrine mechanism. Further studies are needed to elucidate the exact mechanisms in which GLI1 regulates CK17 expression and keratin formation in ameloblastomas.

Based on our results, both the MAPK and SHH pathways may have an impact on the pathogenesis of ameloblastoma because there is a high prevalence of concomitant presence of the *BRAF V600E* mutation and the *GLI1* mRNA and protein overexpression in our ameloblastoma cases. Evidence of a crosstalk between MAPK and SHH pathway and therefore

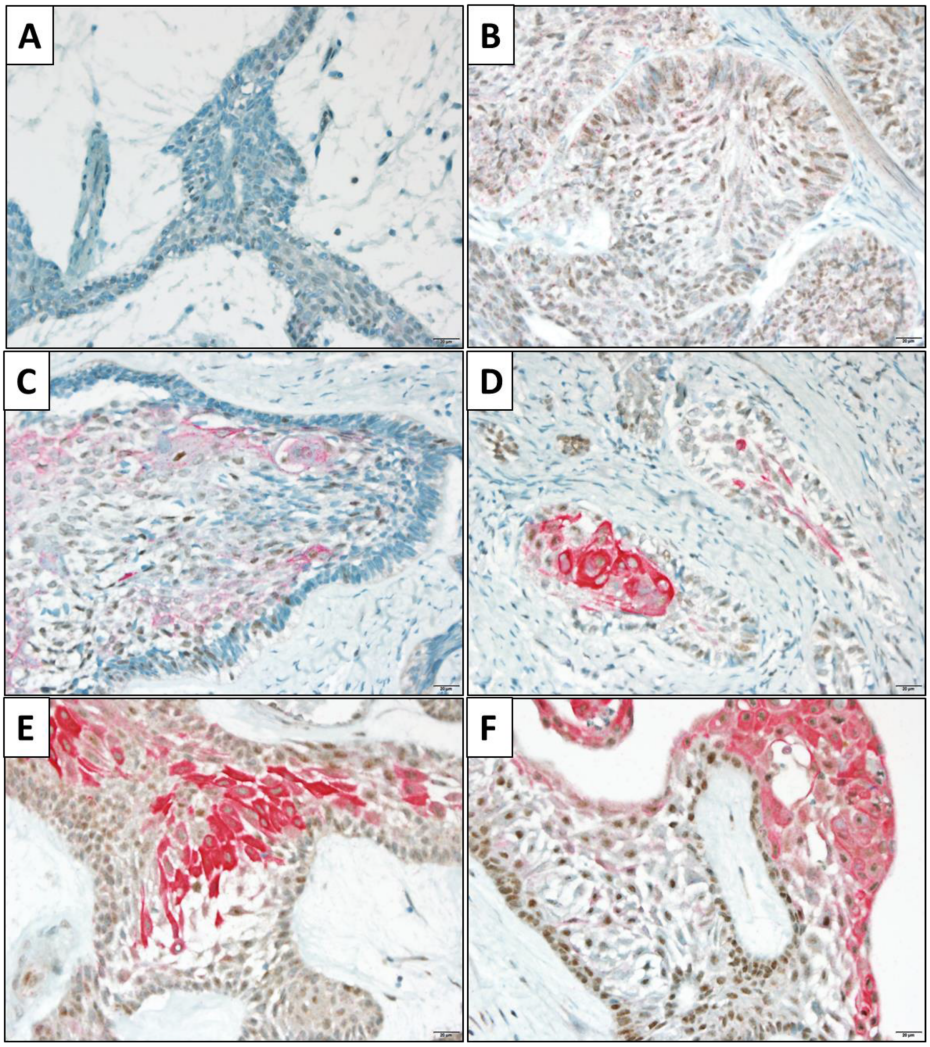

Figure 5 Double immunohistochemical staining for GLI1 protein and CK17 in ameloblastomas. (A) A plexiform ameloblastoma demonstrating scattered GLI1 protein–positive peripheral tumor cells, accompanied by CK17-negative central cells. (B–C) Follicular ameloblastomas showing increased GLI1 protein expression, characterized by brown nuclear staining in the peripheral cells of tumor nests, with weak and focal CK17 red cytoplasmic staining in the central stellate reticulum–like cells. (D–F) Acanthomatous ameloblastomas exhibiting prominent GLI1 protein–positive brown nuclear staining in both peripheral and central tumor cells, together with strong CK17 red cytoplasmic staining in the acanthomatous cells within the tumor nests. (Original magnification: A–F, 400 × .)

affects the treatment outcome has been reported in many tumor types, including skin cancer, melanomas, colon cancers, breast cancers, etc.[25]

In spite of the obvious response to the MAPK pathway inhibitors in treating ameloblastomas, residual diseases are present in these case reports after various durations of mutant-specific targeted therapies,[7–11,26,27] which raises the question of possible drug resistance. Notably, the interactions between the MAPK and SHH pathways and their influences to the prognosis have been well elucidated by many researches in different kinds of neoplasms.[28–31] The drug resistance in ameloblastomas may also arise from crosstalk of the MAPK and SHH pathways. Recent case report[8] and case series[11] have both documented the pathologic findings of squamous differentiation of the tumor from the removed residual ameloblastoma specimen status post BRAF-targeted (dabrafenib) or duo BRAF/MEK inhibitors (dabrafenib/trametinib) therapy, which is possible through the activation of the SHH pathway. This finding also indicates the possibility of concomitant activation of both the MAPK and SHH pathways in ameloblastomas. As the odontogenic keratocyst is recognized for its activation of the SHH pathway,[32–34] with the majority of cases exhibiting identifiable PTCH mutations in both sporadic and syndromic instances,[32] we propose, in parallel with the use of SMO inhibitors in Gorlin syndrome patients, that if resistance to drugs or a suboptimal response is observed in the treated ameloblastomas following the administration of MAPK pathway inhibitors, consideration may be given to block the SHH pathway. This recommendation stems from the frequent coexistence of *GLI1* mRNA and protein overexpression, as well as BRAF mutation, observed in a substantial number of ameloblastomas in Taiwan.

In conclusion, our study demonstrated a frequent concomitant presence of *BRAF V600E* mutation and GLI1 mRNA and protein overexpression, suggesting a potential crosstalk between the MAPK and SHH signaling pathways, particularly in the acanthomatous subtype of ameloblastoma. Moreover, increased *GLI1* mRNA expression is significantly associated with the older patient age, tumor recurrence, and keratin formation, supporting the notion that activation of the SHH pathway may represent a later event in the tumor evolution and may contribute to a more aggressive biological behavior in ameloblastoma.

Declaration of competing interest

The authors have no conflicts of interest relevant to this article.

Acknowledgments

We thank the staff of the Second Core Lab, Department of Medical Research, and Digital slide scanning service in Department of Pathology, National Taiwan University Hospital for technical support during the study. We also thank the Oral Pathology Lab and the staff, Mr. Cheng-Hsueh Lin and Chao-Hung, Cheng, Department of Dentistry, National Taiwan University Hospital for the facility and technical support during the study. This research was funded by Grant 112-M001 from National Taiwan University Hospital Yun Lin Branch to P.H. Lu and Grants 113-S0296, 114-SS0024 from National Taiwan University Hospital and Grant NSTC 112-2314-B-002-090-MY3 from National Science and Technology Council to J.Y.F. Chang.

References

1. Odell EW, Muller S, eds. *WHO classification of tumours. Head and neck tumours*, 5th ed. Lyon (France): International Agency for Research on Cancer, 2023.
2. Neville BW, Damm DD, Allen CM, Chi AC. *Oral and maxillofacial pathology*, 5th ed. St. Louis: Elsevier, 2024:707—16.
3. Brown NA, Betz BL. Ameloblastoma: a review of recent molecular pathogenetic discoveries. *Biomarkers Cancer* 2015; 7(Suppl 2):19—24.
4. Brown NA, Rolland D, McHugh JB, et al. Activating FGFR2-RAS-BRAF mutations in ameloblastoma. *Clin Cancer Res* 2014;20: 5517—26.
5. Chang JYF, Lu PH, Tseng CH, Wang YP, Lee JJ, Chiang CP. Factors affecting the accuracy of anti-BRAF V600E immunohistochemistry results in ameloblastomas. *J Oral Pathol Med* 2023;52:342—50.
6. Sweeney RT, McClary AC, Myers BR, et al. Identification of recurrent SMO and BRAF mutations in ameloblastomas. *Nat Genet* 2014;46:722—5.
7. Kaye FJ, Ivey AM, Drane WE, Mendenhall WM, Allan RW. Clinical and radiographic response with combined BRAF-targeted therapy in stage 4 ameloblastoma. *J Natl Cancer Inst* 2015; 107:378.
8. Tan S, Pollack JR, Kaplan MJ, Colevas AD, West RB. BRAF inhibitor treatment of primary BRAF-mutant ameloblastoma with pathologic assessment of response. *Oral Surg Oral Med Oral Pathol Oral Radiol* 2016;122:e5—7.
9. Abramson Z, Dayton OL, Drane WE, Mendenhall WM, Kaye FJ. Managing stage 4 ameloblastoma with dual BRAF/MEK inhibition: a case report with 8-year clinical follow-up. *Oral Oncol* 2022;128:105854.
10. Grynberg S, Vered M, Shapira-Frommer R, et al. Neoadjuvant BRAF-targeted therapy for ameloblastoma of the mandible: an organ preservation approach. *J Natl Cancer Inst* 2024;116: 539—46.
11. Hirschhorn A, Grynberg S, Campino GA, et al. Histopathologic and molecular insights following the management of ameloblastomas via targeted therapies - pathological and clinical perspectives. *Head Neck Pathol* 2024;18:129.
12. Daws S, Chaiyasate K, Lehal A. Treatment of a BRAF V600E Positive ameloblastoma in a pediatric patient with MEK inhibitor monotherapy. *FACE* 2021;2:179—82.
13. Tseng CH, Lu PH, Wang YP, Chang JYF. Enrichment of SOX2-positive cells in BRAF V600E mutated and recurrent ameloblastoma. *J Personalized Med* 2022;12:77.
14. Schneider CA, Rasband WS, Eliceiri KW. NIH image to ImageJ: 25 years of image analysis. *Nat Methods* 2012;9:671—5.
15. Diniz MG, Gomes CC, Guimaraes BV, et al. Assessment of BRAFV600E and SMOF412E mutations in epithelial odontogenic tumours. *Tumour Biol* 2015;36:5649—53.
16. Kurppa KJ, Caton J, Morgan PR, et al. High frequency of BRAF V600E mutations in ameloblastoma. *J Pathol* 2014;232: 492—8.
17. Lu Y, Xuan M, Takata T, et al. Odontogenic tumors. A demographic study of 759 cases in a Chinese population. *Oral Surg Oral Med Oral Pathol Oral Radiol Endod* 1998;86:707—14.
18. Mosadomi A. Odontogenic tumors in an African population. Analysis of twenty-nine cases seen over a 5-year period. *Oral Surg Oral Med Oral Pathol* 1975;40:502—21.
19. Regezi JA, Kerr DA, Courtney RM. Odontogenic tumors: analysis of 706 cases. *J Oral Surg* 1978;36:771—8.
20. Oh KY, Cho SD, Yoon HJ, Lee JI, Ahn SH, Hong SD. High prevalence of BRAF V600E mutations in Korean patients with ameloblastoma: clinicopathological significance and correlation with epithelial-mesenchymal transition. *J Oral Pathol Med* 2019;48:413—20.
21. Seki-Soda M, Sano T, Ito K, Yokoo S, Oyama T. An immunohistochemical and genetic study of BRAF(V600E) mutation in Japanese patients with ameloblastoma. *Pathol Int* 2020;70: 224—30.
22. Lapthanasupkul P, Laosuk T, Ruangvejvorachai P, Aittiwarapoj A, Kitkumthorn N. Frequency of BRAF V600E mutation in a group of Thai patients with ameloblastomas. *Oral Surg Oral Med Oral Pathol Oral Radiol* 2021;132:e180—5.
23. Gultekin SE, Aziz R, Heydt C, et al. The landscape of genetic alterations in ameloblastomas relates to clinical features. *Virchows Arch* 2018;472:807—14.
24. Mikami Y, Fujii S, Nagata K, et al. GLI-mediated Keratin 17 expression promotes tumor cell growth through the anti-apoptotic function in oral squamous cell carcinomas. *J Cancer Res Clin Oncol* 2017;143:1381—93.
25. Rovida E, Stecca B. Mitogen-activated protein kinases and Hedgehog-GLI signaling in cancer: a crosstalk providing therapeutic opportunities? *Semin Cancer Biol* 2015;35:154—67.
26. Faden DL, Algazi A. Durable treatment of ameloblastoma with single agent BRAFi Re: clinical and radiographic response with combined BRAF-targeted therapy in stage 4 ameloblastoma. *J Natl Cancer Inst* 2017;109:djw190.
27. Hirschhorn A, Campino GA, Vered M, et al. Upfront rational therapy in BRAF V600E mutated pediatric ameloblastoma promotes ad integrum mandibular regeneration. *J Tissue Eng Regen Med* 2021;15:1155—61.
28. Ji Z, Mei FC, Xie J, Cheng X. Oncogenic KRAS activates hedgehog signaling pathway in pancreatic cancer cells. *J Biol Chem* 2007;282:14048—55.

29. Ruddocks LA, Fitzpatrick SG, Bhattacharyya I, Cohen DM, Islam MN. Calcifying epithelial odontogenic tumor: a case series spanning 25 years and review of the literature. *Oral Surg Oral Med Oral Pathol Oral Radiol* 2021;131:684–93.
30. Seto M, Ohta M, Asaoka Y, et al. Regulation of the hedgehog signaling by the mitogen-activated protein kinase cascade in gastric cancer. *Mol Carcinog* 2009;48:703–12.
31. Wei L, Xu Z. Cross-signaling among phosphinositide-3 kinase, mitogen-activated protein kinase and sonic hedgehog pathways exists in esophageal cancer. *Int J Cancer* 2011;129:275–84.
32. Barreto DC, Gomez RS, Bale AE, Boson WL, De Marco L. PTCH gene mutations in odontogenic keratocysts. *J Dent Res* 2000;79:1418–22.
33. Heikinheimo K, Kurppa KJ, Laiho A, et al. Early dental epithelial transcription factors distinguish ameloblastoma from keratocystic odontogenic tumor. *J Dent Res* 2015;94:101–11.
34. Vered M, Peleg O, Taicher S, Buchner A. The immunoprofile of odontogenic keratocyst (keratocystic odontogenic tumor) that includes expression of PTCH, SMO, GLI-1 and bcl-2 is similar to ameloblastoma but different from odontogenic cysts. *J Oral Pathol Med* 2009;38:597–604.